MOLTEN SALT ELECTROLYTES FOR HIGH-TEMPERATURE LITHIUM CELLS*

D. R. VISSERS**, L. REDEY and T. D. KAUN

Chemical Technology Division, Argonne National Laboratory, Argonne, IL 60439-4837 (U.S.A.)

Summary

The composition and melting point of the molten salt electrolyte play a key role in the performance of high-temperature Li-alloy/metal sulfide cells. For example, the performance of the Li–Al/FeS cell operated under flooded-electrolyte conditions improves markedly with an increase in the LiCl content of the LiCl–KCl electrolyte. A similar cell, when operated in a starved-electrolyte state, requires the use of an all-lithium cation electrolyte (*e.g.*, LiF–LiCl–LiBr) to achieve good performance. Both these electrolytes have fairly high melting points, > 400 °C. The Li–Al/FeS$_2$ cell, on the other hand, has been found to operate well as an upper-plateau cell in an electrolyte (25mol%LiCl–37mol%LiBr–38mol%KBr) with a low melting point, 310 °C. Recent laboratory investigations have also demonstrated that the Li–Al/(Ni–Fe)S$_2$ cell operates very well in an Li$_2$S saturated, all-lithium, cation electrolyte at high temperatures, 475 °C.

1. Introduction

The high-temperature lithium cells under study at the Argonne National Laboratory (ANL) utilize either Li–Al, Li–Si, or Li–Al–Si negative electrodes, FeS, FeS$_2$, or (Ni, Fe)S$_2$ positive electrodes, and a molten salt electrolyte [1 - 7]. The cells operate in the temperature range 400 - 475 °C, depending on the electrolyte composition and choice of positive electrode. Previous industrial firms engaged in development of these cells included Eagle-Picher Industries, Inc., Gould Inc., and Rockwell International. At present, Westinghouse Corp. and Argonne National Laboratory (ANL), in a collaborative program, are developing batteries for electric vehicle

---

propulsion using the Li–Al–Si/FeS cell couple, and ANL is developing the Li–Al/FeS$_2$ cell couple to the engineering level.

In the past, the bulk of the research and development effort on the lithium/sulfide cells emphasized the Li–Al/FeS over the Li–Al/FeS$_2$ system because of the poor capacity retention of the Li–Al/FeS$_2$ system and the cost of the current collector materials associated with the FeS$_2$ electrode. However, because the development of the Li–Al/FeS cell couple is at a fairly advanced state, and because the Li–Al/FeS$_2$ system has the potential of yielding cells with much higher specific energy and power than those obtainable with the Li–Al/FeS system, the disulfide cell is now receiving greater attention.

In the paper we will review the importance of the molten salt electrolyte in the performance of the Li–Al/FeS and the Li–Al/FeS$_2$ systems and will discuss the recent breakthrough in capacity retention achieved with the latter system. Since the effect of the electrolyte composition on the performance of the lithium-alloy electrodes is not as pronounced as it is on the performance of the metal sulfide electrodes of the respective cell systems, this review will only address the effect of electrolyte on the performance of the FeS and FeS$_2$ electrode systems.

2. Electrolyte and FeS electrode performance

The chemistry and electrochemistry of the FeS electrode have been investigated in detail [3, 4, 8 - 20], and the results indicate that the electrode reactions are more complex than earlier thought. For example, the Li–Fe–S phase diagram (Fig. 1) suggests two reactions:
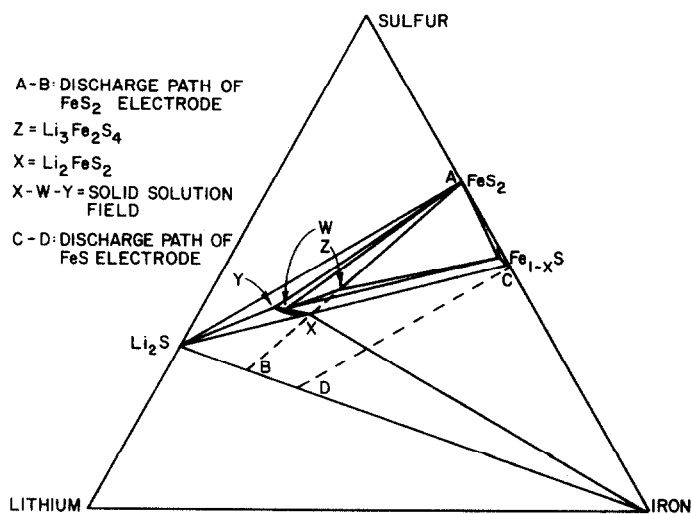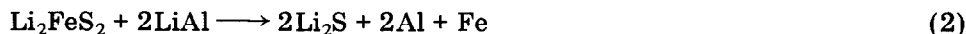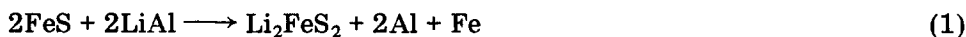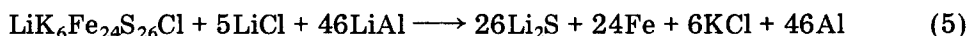

Fig. 1. Phases in the Li–Fe–S system at 450 °C.

$$2FeS + 2LiAl \longrightarrow Li_2FeS_2 + 2Al + Fe \qquad (1)$$

$$Li_2FeS_2 + 2LiAl \longrightarrow 2Li_2S + 2Al + Fe \qquad (2)$$
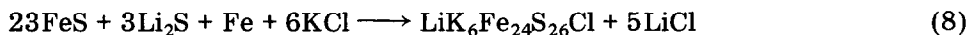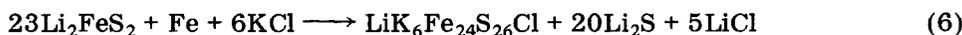
These two reactions should appear essentially as one on the discharge voltage plateau, since the Gibbs energy of formation of Li_2FeS_2 from FeS and Li_2S is less than 1 kcal mol^{-1} [8]. However, microscopic examination of the phases present in the electrode after being cycled in the LiCl–KCl eutectic electrolyte at temperatures to 450 °C indicated that the major voltage plateau corresponds to the formation of J-phase ($LiK_6Fe_{24}S_{26}Cl$) [8, 10, 18]. The J-phase is formed in the electrode by an interaction of the electrolyte with the active materials in the FeS electrode. Thus, in addition to the above two reactions, three other electrochemical and four chemical reactions have been identified [3]:

Electrochemical reactions

$$26FeS + 6KCl + 6LiAl \longrightarrow 2Fe + LiK_6Fe_{24}S_{26}Cl + 5LiCl + 6Al \qquad (3)$$

$$LiK_6Fe_{24}S_{26}Cl + 5LiCl + 20LiAl \longrightarrow 13Li_2FeS_2 + 11Fe + 6KCl + 20Al \qquad (4)$$

$$LiK_6Fe_{24}S_{26}Cl + 5LiCl + 46LiAl \longrightarrow 26Li_2S + 24Fe + 6KCl + 46Al \qquad (5)$$

Chemical reactions

$$23Li_2FeS_2 + Fe + 6KCl \longrightarrow LiK_6Fe_{24}S_{26}Cl + 20Li_2S + 5LiCl \qquad (6)$$

$$3Li_2FeS_2 + 20FeS + Fe + 6KCl \longrightarrow LiK_6Fe_{24}S_{26}Cl + 5LiCl \qquad (7)$$

$$23FeS + 3Li_2S + Fe + 6KCl \longrightarrow LiK_6Fe_{24}S_{26}Cl + 5LiCl \qquad (8)$$

$$FeS + Li_2S \longrightarrow Li_2FeS_2 \qquad (9)$$
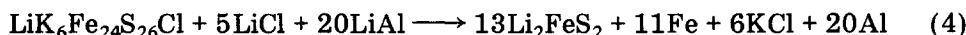
This phase transition sequence, as well as e.m.f. and thermodynamic information on these reactions, was determined by Tomczuk *et al.* [3].

During the development of the FeS cell, it became evident that the formation of J-phase, which occurs through reactions with the KCl in the LiCl–KCl electrolyte, hinders the kinetics of the FeS electrode. At one time, Cu_2S was added to the positive electrode to inhibit the formation of this phase, but subsequent post-test examinations of the cells indicated that it tended to cause early cell failures because of the precipitation of metallic copper in the electrode separators, which resulted in short circuits [14]. Small-scale cell tests [10] and thermodynamic studies indicated that the stability of this phase can be decreased either by increasing the LiCl content of the electrolyte (above the eutectic) or by raising the operating temperature of the cell. Saboungi and Martin [15] made a careful metallographic examination of the products of reactions (6) and (7) in eutectic and LiCl-saturated electrolyte to determine the temperature above which J-phase does not form. For reaction (6), the temperatures are 455 °C for the eutectic electrolyte and 419 °C for the LiCl-saturated electrolyte. The temperatures for reaction (7) are 623 °C for the eutectic and 481 °C

for the LiCl-saturated electrolyte. Small-scale FeS cell tests by Vissers *et al.* [20] indicated that, as the LiCl content of the electrolyte increases, the active material utilization of the FeS electrodes improves markedly and the effect of temperature on the electrode utilization decreases (see Table 1). From these studies, an LiCl–KCl electrolyte containing ~67 mol% LiCl seemed appropriate for Li–Al/FeS cell development.

The formation of $LiK_6Fe_{24}S_{26}Cl$ can be entirely avoided by the use of an electrolyte that contains only lithium cations, *e.g.*, LiF–LiCl–LiBr. Although cell performance can be improved considerably by increasing the lithium ion content of the electrolyte (either by increasing the LiCl concentration or by employing an all-lithium-cation electrolyte), the increased lithium content in these electrolytes results in a higher liquidus temperature or melting point for the electrolyte. Consequently, the cell operating temperature must be raised above 450 °C. Eagle-Picher and ANL used the LiCl-rich electrolyte (68mol%LiCl–32mol%KCl) in their cells, whereas Gould Inc. (now Westinghouse) used the all-lithium-cation electrolyte (22mol%LiF–32mol%LiCl–46mol%LiBr).

Because low-carbon steel current collectors are used in engineering cells, the normal charge cutoff voltages are always less than 1.60 V *versus* LiAl to minimize the oxidation of the current collector to $FeCl_2$. The soluble $FeCl_2$ tends to be reduced by the dissolved lithium metal in the electrolyte and results in metallic iron deposits in the separator. With time,

TABLE 1

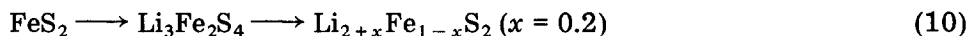Utilization of positive electrode in LiAl/LiCl–KCl/FeS cells

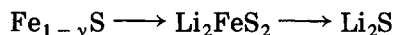| LiCl concentration (mol%)	Temp. (°C)	Current density (mA cm^{-2})		FeS electrode utilization (%)
		Charge	Discharge	
53	450	50	50	25
	500	50	50	44
	450	100	100	14
	500	100	100	40
58[a]	450	50	50	52
	500	50	50	70
	450	100	100	44
	500	100	100	55
63	450	50	50	74
	500	50	50	77
	450	100	100	68
	500	100	100	71
67	450	50	50	91
	500	50	50	90
	450	100	100	85
	500	100	100	86

[a]Eutectic composition.

short circuits are caused by these deposits and result in cell failure. Such deposits are the cause of the failure in most Li–Al/FeS engineering cells. When one shifts from lithium electrolytes that contain only chloride ions to electrolytes that also contain bromide ions, the formation of soluble iron bromide, being less thermodynamically stable than that of iron chloride, tends to form at lower positive electrode potential. Therefore, when operating such cells, the use of lower charge cutoff voltages tends to be beneficial.
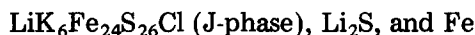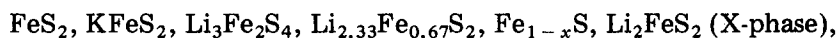
3. Electrolyte and the FeS$_2$ electrode performance

The bulk of work on characterization of FeS$_2$ electrode performance has been carried out using the LiCl–KCl eutectic electrolyte (m.p. 352 °C). In this review, the information presented is for the eutectic electrolyte unless stated otherwise. The first reported studies on the FeS$_2$ electrode indicated good electrochemical properties [1]. Since then, many studies have been performed to establish the phases formed and the phase progression as this electrode is discharged at cell operating temperatures [8, 21 - 28]. Martin established the Li–Fe–S phase diagram that relates to the FeS and FeS$_2$ electrode phase transitions at 450 °C (see Fig. 1). The phases were identified in out-of-cell preparations examined by metallographic and X-ray diffraction techniques. Martin's phase diagram work indicates the phase progression sequence as

$$FeS_2 \longrightarrow Li_3Fe_2S_4 \longrightarrow Li_{2+x}Fe_{1-x}S_2 \ (x = 0.2) \tag{10}$$

and

$$Fe_{1-y}S \longrightarrow Li_2FeS_2 \longrightarrow Li_2S$$

Cycled FeS$_2$ electrodes examined by Tomczuk et al. [8] for phase identification indicated the following phases:

$$FeS_2, KFeS_2, Li_3Fe_2S_4, Li_{2.33}Fe_{0.67}S_2, Fe_{1-x}S, Li_2FeS_2 \ (\text{X-phase}),$$

$$LiK_6Fe_{24}S_{26}Cl \ (\text{J-phase}), Li_2S, \text{ and Fe}$$

The data of Tomczuk and Martin are in good agreement, with the exception of the solid solution phase, $Li_{2+x}Fe_{1-x}S_2$, which was not detected because the phase decomposes on cooling to yield $Li_{2.33}Fe_{0.67}S_2$ and Li_2FeS_2 and, of course, the two potassium-containing phases. The potassium-containing phases are always minor phases in the FeS$_2$ electrode. Coulometry studies [8] of the FeS$_2$ electrode provided additional support for Martin's phase diagram, since breaks in the curve of voltage *versus* depth of discharge were observed very near to the composition values predicted by the phase diagram. The X-ray diffraction patterns for the respective phases were determined and have been published [4].

The phase progression in cells charged at 18 mA cm^{-2} to a preselected voltage and then constant-voltage charged at this value was consistent with the phase diagram data [4] (see Table 2). In these experiments, however,

TABLE 2

Sulfide phases observed during charge of $LiAl/FeS_2$ cells operated at 410 °C using eutectic electrolyte[a]

Charge potential[b] vs. $(\alpha + \beta)$ LiAl	X-ray findings		Metallographic findings
	Major phase	Minor phase	
1.53	Li_2FeS_2	$LiK_6Fe_{24}S_{26}Cl$	Li_2FeS_2 + trace of $LiK_6Fe_{24}S_{26}Cl$
1.64	$Li_{2.33}Fe_{0.67}S_2$ and Li_2FeS_2	$Fe_{1-x}S$	Li_2FeS_2 + $Fe_{1-x}S$ + $Li_{2.33}Fe_{0.67}S_2$
1.72	$Li_3Fe_2S_4$	None detected	$Li_3Fe_2S_4$ only
1.79	$Li_3Fe_2S_4$	None detected	$Li_3Fe_2S_4$ + 5%$Fe_{1-x}S$
1.82	$Li_3Fe_2S_4$	$FeS_2 + Fe_{1-x}S$	Not examined
1.85	FeS_2	$Fe_{1-x}S$	$FeS_2 + Fe_{1-x}S$

[a]Li_2S and Fe react at lower potential (1.33 V) to form Li_2FeS_2.
[b]Constant current charge at ~ 18 mA cm^{-2} followed by > 18 h constant voltage charge (final current density < 2 mA cm^{-2}).

FeS_2 formation did not occur at the voltage at which it was observed when these cells were discharged, namely, 1.76 V at 400 °C. Instead, complete formation of FeS_2 was not observed until a value of ~ 1.85 V was reached. Cyclic voltammetry experiments carried out by Preto et al. [28] also indicated a nucleation overpotential of 95 mV for the formation of FeS_2 at 400 °C. Preto et al. were able to show that the value of the nucleation overpotential depended on the degree of discharge. For example, when the FeS_2 electrode had been partially discharged to $Li_3Fe_2S_4$, with some FeS_2 still present in the electrode, the nucleation overpotential dropped to only 20 mV. Metallographic examinations on cycled electrodes [4] indicated that FeS_2 did not form on $Li_3Fe_2S_4$ but had formed on $Fe_{1-x}S$ particles. Since $Li_3Fe_2S_4$ particles were always observed on FeS_2 particles on discharge, these workers concluded that charge and discharge reactions were quite different in the $Li_3Fe_2S_4 \rightleftharpoons FeS_2$ transition region. Support for this conclusion was also obtained by Preto et al. [28] who were able to show that a nonequilibrium soluble species is formed in the region where $Li_3Fe_2S_4$ disappears and FeS_2 is formed. Although this species could not be conclusively identified, it was believed to be Li_2S_2. Earlier, Schmidt and Weppner [29], in a study of the kinetic properties of the ternary Li–Fe–S phases, also claimed that Li_2S_2 is formed in FeS_2 electrodes, but did not give any proof for this claim. More recent work by Redey [30] suggests that excess Li_2S in the cell electrolyte enhances the charging characteristics of the FeS_2 electrode. This is thought to be due to the formation of soluble lithium polysulfide species which chemically react with $Li_3Fe_2S_4$ to form FeS_2.

To determine how the composition of the LiCl–KCl electrolyte affected the formation of FeS_2, Preto *et al.* [28] conducted cyclic voltammetry studies using, in addition to the eutectic composition, an LiCl-rich electrolyte (61mol%LiCl–39mol%KCl) and a KCl-rich electrolyte (55mol%-LiCl–45mol%KCl). The results of the studies (see Fig. 2) indicated that increasing the LiCl content of the electrolyte had only a very slight affect on the nucleation overpotential but tended to sharpen the upper plateau portion of the voltammogram and to lower the voltage required to complete the reaction. In the KCl-rich electrolyte, the upper plateau portion of the voltammogram was split into two separate peaks, and the electrochemical reactions for the respective peaks were believed to be:

$$Li_3Fe_2S_4 + Al + 2KCl \longrightarrow 2KFeS_2 + LiAl + 2LiCl \tag{11}$$

$$KFeS_2 + Al + LiCl \longrightarrow FeS_2 + LiAl + KCl \tag{12}$$

The voltage required to complete reaction (12) was very similar to that observed in the LiCl–KCl eutectic electrolyte. Similar cyclic voltammetry studies carried out by Wang and Seefurth [31] indicated that the overpotential of the FeS_2 formation reaction is usually proportional to the activity of lithium ions in the electrolyte.

Recently, Kaun [32, 33] found that the FeS_2 electrode, when operated in LiCl-rich electrolyte (25mol%LiCl–37mol%LiBr–38mol%KBr) behaved very much like one operated in LiCl-rich (61mol%LiCl–39mol%KCl) electrolyte, as reported by Preto *et al.* [28]. This suggests that the kinetics of the FeS_2 formation reaction is enhanced by the lower levels of potassium ions in the system. Whether or not these observations are related to the formation of $KFeS_2$ in the FeS_2 electrode during charging is not certain, but the observations suggest this might well be the case.

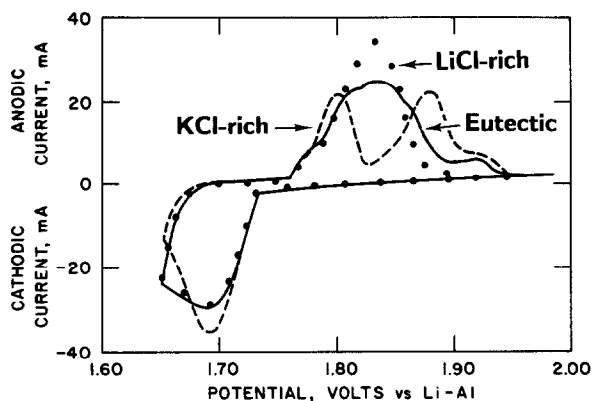Fig. 2. Voltammogram of FeS_2 upper-plateau electrode in LiCl–KCl electrolyte systems, 425 °C.

4. Breakthroughs in Li–Al/FeS$_2$ cell system

The Li–Al/FeS$_2$ and Li–Si/FeS$_2$ cells that use the LiCl–KCl eutectic electrolyte and operate at 425 - 450 °C have exhibited very poor capacity retention. This poor capacity retention appears to be related to the irreversibility of the FeS$_2$ formation reaction discussed in Section 3 of this paper and to the formation of soluble species during the FeS$_2$ formation reaction. Small amounts of sulfur may also be lost from the FeS$_2$ electrodes by volatilization at the higher temperatures.

Recently, several major breakthroughs have resulted in Li–Al/FeS$_2$ cells that have excellent capacity retention [13]. In the first case, unlike the earlier Li–Al/FeS$_2$ cells that utilized the LiCl–KCl eutectic (m.p. 352 °C) and operated on both FeS$_2$ electrode plateaux (FeS$_2 \rightarrow$ Li$_2$FeS$_2 \rightarrow$ Li$_2$S + Fe), these improved cells were operated only on the upper plateau (FeS$_2 \rightarrow$ Li$_2$FeS$_2$) and utilized a low melting electrolyte (25mol%LiCl–37mol%LiBr–38mol%KBr, m.p. 310 °C). Cell testing has shown that these cells exhibit very high specific energy and power and very stable capacity with extended cycling. Why these cells have excellent capacity retention, unlike the earlier cells, is not completely understood, but it very probably results from a combination of effects. First, the cells are operated at a lower temperature, reducing the solubility of any harmful soluble species formed. Second, the broad liquidus region of the LiCl–LiBr–KBr electrolyte permits significant electrolyte composition changes (Li$^+$/K$^+$ ratio of 1.25 - 1.81) without salt precipitation; thus, one can operate the FeS$_2$ electrode with active material loading densities of 50vol% solids in the fully charged state, which also reduces transport of any soluble transition metal species from the electrode. Third, on the upper plateau, the FeS$_2$ electrode is reported [3] to be more reversible in this electrolyte than in the LiCl–KCl electrolyte, where the higher Li$^+$ ion content of the electrolyte tends to eliminate K$^+$-ion-containing electrode phases, such as LiK$_6$Fe$_{23}$S$_{26}$Cl and KFeS$_2$, which tend to interfere with the kinetics of FeS$_2$ formation.

A second metal disulfide electrode that has demonstrated excellent capacity retention in small cell tests is the NiS$_2$–FeS$_2$ electrode saturated with Li$_2$S [34 - 36]. This electrode has been operated in both the LiF–LiCl–LiBr electrolyte (m.p. 445 °C) at 465 °C and in the LiCl–LiBr–KBr electrolyte at 400 °C. Unlike the upper-plateau FeS$_2$ electrode described earlier, in which electrode thermal instability has been alleviated, this electrode compensates for sulfur loss by operating with an electrolyte saturated with Li$_2$S. Cells constructed with these Li$_2$S-saturated metal disulfide electrodes appear to have good cycle life and may be operated on both plateaux and also seem to be insensitive to cell overcharge.

5. Electrolyte and power performance

The power performance of a cell is greatly influenced by the composition of the electrolyte. According to the routine practice of the Argonne
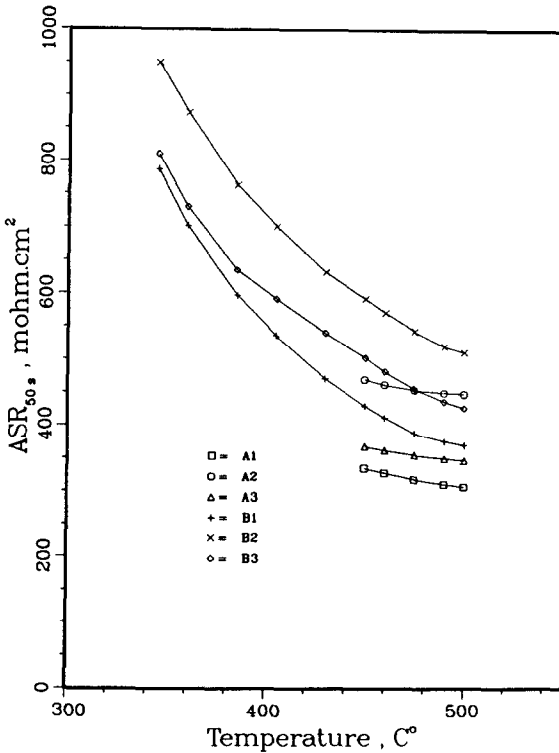
Fig. 3. Effects of electrolyte composition and temperature on area-specific impedance measured in the 50th second of 1 A cm^{-2}-intensity current pulses. A, Li$_2$S-saturated all-Li$^+$-cation electrolyte; B, Li$_2$S-saturated low-melting electrolyte. 1, 2, and 3 refer to approximate utilizations of the electrode: 5, 25 and 80%, respectively.

National Laboratory, the power performance is quantified by either the area-specific impedance (ASR$_t$) or the area-specific peak-power (ASPP$_t$) of the cell. The t subscript indicates the interrupt or pulse time as used in the measurement of the two quantities. Figure 3 shows the ASI$_{50s}$ values of an (Fe–Ni)S$_2$ electrode as a function of temperature. The ASI$_{50s}$ values were measured for this electrode in LiF–LiCl–LiBr and LiCl–LiBr–KBr electrolytes at three utilizations. Lower ASI$_t$ values were measured in the all-Li$^+$ electrolyte, indicating a better power capability of a cell when built with this electrolyte. The effect of temperature on ASI$_t$ is small in this electrolyte, but the operational range is rather narrow because of the high melting point and the thermal-stability problems of the metal sulfides above 500 °C. Although impedance substantially increases with decreasing temperature in the LiCl–LiBr–KBr electrolyte, the ASI$_{50s}$ = 600 - 800 ohm cm^2 values indicate acceptable performance, even at 380 °C.

   Power performance of a cell is greatly influenced by the electrolyte composition [30]. Figure 4 indicates sustained area-specific peak power
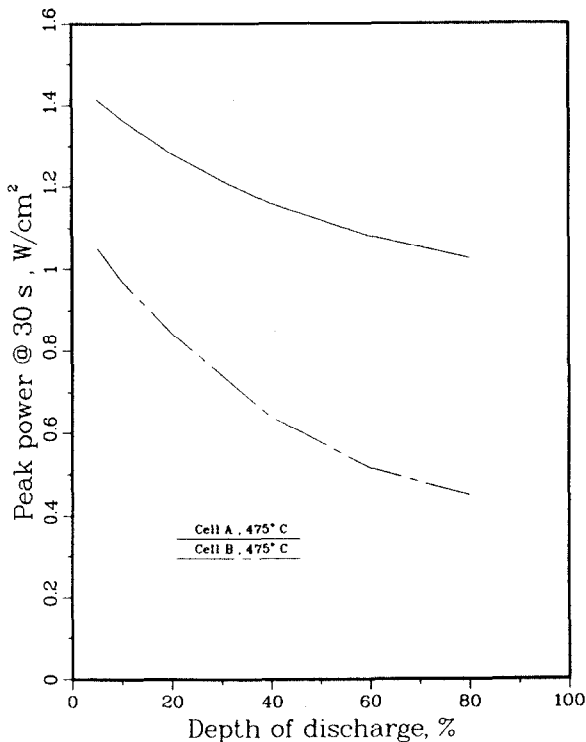
Fig. 4. Peak-power performance of LiAlSi/(FeNi)S_2 cells in (A) all-Li$^+$-cation and (B) low-melting electrolytes.

at 30 s (ASPP$_{30s}$) for an LiAlSi/(Fe–Ni)S_2 cell tested with both the LiF–LiCl–LiBr and LiCl–LiBr–KBr electrolytes. The all-Li$^+$ electrolyte results in much better power performance.

6. Conclusions

Cell studies have clearly shown that the electrolyte plays a key role in the performance and capacity retention of lithium-alloy/iron sulfide cells. The chemistry of the FeS electrode, for example, may be greatly affected by interactions between the electrolyte and the active electrode materials, where the formation of J-phase can greatly slow the kinetics of the charge–discharge reactions. Increasing the lithium-ion activity of the electrolyte was found to have a marked effect on reducing the formation of J-phase. The use of a low melting electrolyte, when blended with an upper-plateau FeS$_2$ electrode, has been shown to stabilize capacity retention in Li–Al/FeS$_2$ cells. Addition of excess Li$_2$S to positive electrodes containing 1:1 blends of NiS$_2$ and FeS$_2$ in either the LiCl–LiBr–KBr or the LiF–LiCl–LiBr electrolyte also appears to stabilize capacity retention of

the cell, even when operated on both major FeS$_2$ plateaux. The power characteristics of the Li–Al/MS$_2$ cells are also markedly affected by the electrolyte composition. While the exact role that the electrolyte plays in the FeS$_2$ electrode system is not completely understood, its importance to the performance and capacity retention of the electrode cannot be underestimated. Further studies are still needed to understand the role of the electrolyte in the LiAl/FeS$_2$ cell system better.

Acknowledgement

References

1 D. R. Vissers, Z. Tomczuk and R. K. Steunenberg, *J. Electrochem. Soc.*, *121* (1974) 655.
2 C. J. Wen, B. A. Baukamp, R. A. Huggins and W. Weppner, *J. Electrochem. Soc.*, *126* (1979) 2258.
3 Z. Tomczuk, S. K. Preto and M. F. Roche, *J. Electrochem. Soc.*, *128* (1981) 760.
4 Z. Tomczuk, B. Tani, N. C. Otto, M. F. Roche and D. R. Vissers, *J. Electrochem. Soc.*, *129* (1982) 925.
5 R. Pollard and J. Newman, *J. Electrochem. Soc.*, *128* (1981) 503.
6 Z. Tomczuk and D. R. Vissers, *J. Electrochem. Soc.*, *133* (1986) 2505.
7 D. R. Vissers, Z. Tomczuk, L. Redey and J. E. Battles, High-temperature lithium-alloy/iron sulfide batteries, in R. O. Bach (ed.), *Lithium: Current Applications in Science, Medicine and Technology*, Wiley, New York, 1985, Ch. 10, pp. 121 - 154.
8 Z. Tomczuk, M. F. Roche and D. R. Vissers, *J. Electrochem. Soc.*, *128* (1981) 2255.
9 Z. Tomczuk, A. E. Martin and R. K. Steunenberg, Chemistry of the FeS electrode of Li/FeS cells, *Ext. Abstr. Electrochem. Soc. Meeting*, *76-2* (1976) 131.
10 B. Tani, *Am. Mineral.*, *62* (1977) 819.
11 C. Melendres and B. Tani, *J. Phys. Chem.*, *82* (1978) 2850.
12 M. L. Saboungi, J. J. Mar and M. Blander, *J. Electrochem. Soc.*, *125* (1978) 1567.
13 M. L. Saboungi and A. E. Martin, Electrochemical and metallographic investigations of the stability of the J (LiK$_6$Fe$_{24}$S$_{26}$Cl) phase in several molten salt mixtures, *Ext. Abstr. Electrochem. Soc. Meeting*, *78-2* (1978) 919.
14 C. E. Vallet and J. Braunstein, *J. Electrochem. Soc.*, *125* (1978) 1193.
15 R. Sharma, *J. Electrochem. Soc.*, *123* (1976) 448.
16 H. F. Gibbard, *J. Electrochem. Soc.*, *125* (1978) 353.
17 D. M. Chen and H. F. Gibbard, *J. Electrochem. Soc.*, *130* (1983) 1975.
18 F. C. Mrazek and J. E. Battles, *J. Electrochem. Soc.*, *124* (1977) 1556.
19 N. C. Otto and J. E. Battles, in High-performance batteries for electric-vehicle propulsion and stationary energy storage, *Argonne Nat. Lab. Rep. ANL-79-39*, May, 1979, 49.
20 D. R. Vissers, K. E. Anderson, C. K. Ho and H. Shimotake, in S. Gross (ed.), *Proc. Symp. on Battery Design and Optimization, Electrochem. Soc. Proc. 79-1* (1979) 416.
21 A. E. Martin, R. K. Steunenberg and Z. Tomczuk, Changes in the composition of FeS$_2$ electrodes of Li/LiCl–KCl/FeS$_2$ cells during cycling, *Ext. Abstr. Electrochem. Soc. Meeting*, *74-2* (1974) 132.

22 A. Rabenaw, B. Schoch and W. Weppner, Molten salt electrochemistry for high-temperature thermochemistry and kinetics of system Li–Fe–S, *Ext. Abstr. Electrochem. Soc. Meeting, 87-2* (1987) 2165.
23 K. Abe and T. Chiku, *J. Electrochem. Soc., 122* (1975) 1322.
24 R. Brec and A. Dugast, *Mater. Res. Bull., 15* (1980) 619.
25 A. E. Martin and Z. Tomczuk, in High-performance batteries for electric-vehicle propulsion and stationary energy storage, *Argonne Nat. Lab. Rep. ANL-79-39,* 1979, p. 71.
26 Z. Tomczuk, B. Tani, N. C. Otto, M. F. Roche and D. R. Vissers, *J. Electrochem. Soc., 129* (1982) 925.
27 A. E. Martin, in High-performance batteries for electric-vehicle propulsion and stationary energy storage, *Argonne Nat. Lab. Rep. ANL-78-84,* 1980, p. 167.
28 S. K. Preto, Z. Tomczuk, S. von Winbush and M. F. Roche, *J. Electrochem. Soc., 130* (1983) 264.
29 J. A. Schmidt and W. Weppner, Kinetics of compositional variations in the ternary system Li–Fe–S, *Ext. Abstr. Electrochem. Soc. Meeting, 82-1* (1982) 562.
30 L. Redey, Power performance of LiAlSi/(FeNi)S$_2$ cells, Proc. First Int. Workshop on High-Temperature Molten Salt Batteries, Argonne, IL, April 16 - 18, 1986, *Argonne Nat. Lab. Rep. ANL-86-40, 1988,* p. B-131.
31 S. S. Wang and R. N. Seefurth, *J. Electrochem. Soc., 134* (1987) 530.
32 T. Kaun, *J. Electrochem. Soc., 132* (1985) 3063.
33 T. Kaun, *Proc. 21st IECEC, August 25 - 29, San Diego, CA, 1986,* p. 1043.
34 T. Kaun, *Proc. Joint Int. Symp. on Molten Salts, Electrochem. Soc. 87-7* (1987) p. 621.
35 T. Kaun, L. Redey and P. Nelson, *Proc. 22nd IECEC, Philadelphia, PA, 1987,* p. 1085.
36 L. Redey, *Proc. 22nd IECEC, Philadelphia, PA, 1987,* p. 1091.